Synthesis and Structures of New Ternary Aluminum Chalcogenides: $LiAlSe_2$, α-$LiAlTe_2$, and β-$LiAlTe_2$

Joonyeong Kim and Timothy Hughbanks*

Department of Chemistry, Texas A&M University, P.O. Box 30012, College Station, Texas 77842-3012

Received February 25, 2000

The synthesis and crystal structures of new ternary aluminum chalcogenides, $LiAlSe_2$, α-$LiAlTe_2$, and β-$LiAlTe_2$, are reported. These compounds are synthesized by solid-state reaction at 800 °C. The single-crystal X-ray structures of these compounds have been determined. $LiAlSe_2$: $a = 6.8228(9)$ Å, $b = 8.266(1)$ Å, $c = 6.5236(7)$ Å, $Pna2_1$ (No. 33, $Z = 4$). α-$LiAlTe_2$: $a = 6.5317(4)$ Å, $c = 11.6904(9)$ Å, $I\bar{4}2d$ (No. 122, $Z = 4$). β-$LiAlTe_2$: $a = 4.4810(6)$ Å, $c = 7.096(1)$ Å, $P3m1$ (No. 156, $Z = 1$). These ternary compounds are formed by fusion of AlQ_4 (Q = Se, Te) tetrahedra. $LiAlSe_2$ shows β-$NaFeO_2$ structure type, which can be viewed as a wurtzite superstructure. α-$LiAlTe_2$ adopts chalcopyrite structure type. In $LiAlSe_2$ and α-$LiAlTe_2$, AlQ_4 (Q = Se, Te) tetrahedra share four corners to build three-dimensional structures and Li atoms are located in the tetrahedral sites between the chalcogen layers. β-$LiAlTe_2$ has polar layers formed by three-corner shared $AlTe_4$ tetrahedra, and Li cations are in the distorted antiprisms between the layers. ^{7}Li MAS NMR studies show that chemical shifts of Li in these ternary chalcogenides are nearly identical regardless of different chemical environments.

Introduction

Ternary chalcogenides with the general formula $A^IM^{III}Q_2$ (A = Li, Cu, Ag; M = Al, Ga, In; Q = S, Se, Te) are usually semiconductors with energy gaps that vary between 0.9 and 4.0 eV. These materials have attracted much attention because of their optoelectronic applications in light emitting diodes (LED), detectors, solar energy converters, and nonlinear optical (NLO) devices.[1−15] These ternary compounds usually crystallize in tetragonal chalcopyrite ($CuFeS_2$) or orthorhombic β-$NaFeO_2$ structure types.[16−22] Both structures incorporate tetrahedral building blocks that share four corners to form three-dimensional nets; the only difference is the stacking sequence of anions. As a result, β-$NaFeO_2$ can be viewed as a wurtzite superstructure based on hexagonal closed stacking of oxygen, whereas the chalcopyrite ($CuFeS_2$) structure is regarded as a zinc blende (ZnS) superstructure in which sulfur atoms have a cubic closed packing eutaxy.

Most research has focused on compounds containing Cu or Ag as the monovalent cation, A^I. Much less is known about ternary lithium chalcogenides perhaps because of crystal growth difficulties and air sensitivity of this class of compounds. However, ternary lithium chalcogenides are also of interest because they have larger energy gaps than corresponding coinage metal compounds and are potentially suitable for birefringent crystals.[23−26] This motivated the synthesis and characterization of ternary lithium chalcogenides of gallium and indium such as $LiGaQ_2$ (Q = S, Se) and $LiInQ_2$ (Q = S, Se, Te), but knowledge of the corresponding ternary aluminum chemistry is lacking.[21−25] Several classes of ternary aluminum chalcogenides were reported: A_3AlQ_3 (A = Na, K; Q = S, Se, Te), $AAlQ_2$ (A = Na for Q = Se, Te; A = K for Q = Te), and $KAlQ_2$ (Q = Se, Te).[27−35] Isolated [$AQ_3 = A_2Q_4Q_{4/2}$] dimers

* To whom correspondence should be addressed. E-mail: trh@mail.chem.tamu.edu. Phone: (979) 845-0125. Fax: (979) 847-8860.

(1) Rincón, C.; Wasim, S. M.; Marín, G.; Huntzinger, J. R.; Galibert, J.; Zwick, A. *Mater. Lett.* **1999**, *38*, 305−307.
(2) Rincón, C.; Hernandez, E.; Wasim, S. M.; Molina, I. *J. Phys. Chem. Solids* **1998**, *56*, 1015−1019.
(3) Marín, G.; Rincón, C.; Wasim, S. M.; Power, C.; Peréz, G. S. *J. Appl. Phys.* **1997**, *81*, 7580−7583.
(4) Soliman, H. S. *J. Phys. D: Appl. Phys.* **1998**, *31*, 1516−1521.
(5) Bottomley, D. J.; Mito, A.; Niki, S.; Yamada, A. *J. Appl. Phys.* **1997**, *82*, 817−824.
(6) Bottomley, D. J.; Mito, A.; Fons, P. J.; Niki, S.; Yamada, A. *IEEE J. Quantum Electron.* **1997**, *33*, 1294−1298.
(7) Jackson, A. G.; Ohmer, M. C.; LeClair, S. R. *Infrared Phys. Technol.* **1997**, *38*, 233−244.
(8) Meng, Q.-B.; Xiao, C.-Y.; Wu, Z.-J.; Feng, K.-a.; Lin, Z.-D.; Zhang, S.-Y. *Solid State Commun.* **1998**, *107*, 369−371.
(9) Brandit, G.; Räuber, A.; Schneider, J. *Solid State Commun.* **1973**, *12*, 481−483.
(10) Robbins, M.; Lambrecht, V. G., Jr. *Mater. Res. Bull.* **1973**, *8*, 703−710.
(11) Lambrecht, V. G., Jr. *Mater. Res. Bull.* **1973**, *8*, 1383−1388.
(12) Robbins, M.; Phillips, J. C.; Lambrecht, V. G., Jr. *J. Phys. Chem. Solids* **1973**, *34*, 1205−1209.
(13) Robbins, M.; Lambrecht, V. G., Jr. *J. Solid State Chem.* **1975**, *15*, 167−170.
(14) Boyd, G. D.; Kasper, H. M.; McFee, J. H. *J. Appl. Phys.* **1973**, *44*, 2809−2812.
(15) Negran, T. J.; Kasper, H. M.; Glass, A. M. *Mater. Res. Bull.* **1973**, *8*, 743−748.
(16) Hoppe, R. *Bull. Soc. Chim. Fr.* **1965**, 1115−1121.
(17) Hahn, V. H.; Frank, G.; Klingler, W.; Meyer, A.-D.; Störger, G. *Z. Anorg. Allg. Chem.* **1953**, *271*, 153−170.
(18) Abrahams, S. C.; Berstein, J. L. *J. Chem. Phys.* **1973**, *59*, 1625−1629.
(19) Abrahams, S. C.; Berstein, J. L. *J. Chem. Phys.* **1973**, *59*, 5415−5422.
(20) Abrahams, S. C.; Berstein, J. L. *J. Chem. Phys.* **1974**, *61*, 1140−1146.
(21) Hönle, W.; Kühn, G.; Neumann, H. *Z. Anorg. Allg. Chem.* **1986**, *532*, 150−156.
(22) Hönle, W.; Kühn, G.; Neumann, H. *Z. Anorg. Allg. Chem.* **1986**, *543*, 161−168.
(23) Kamijoh, T.; Kuriyama, K. *J. Cryst. Growth* **1979**, *46*, 801−803.
(24) Kuriyama, K.; Nozaki, T. *J. Appl. Phys.* **1981**, *52*, 6441−6443.
(25) Kamijoh, T.; Kuriyama, K. *J. Cryst. Growth* **1981**, *51*, 6−10.
(26) Kamijoh, T.; Kuriyama, K. *J. Appl. Phys.* **1981**, *52*, 1102−1103.
(27) Weis, J.; Schäfer, H.; Schön, G. *Z. Naturforsch.* **1976**, *31b*, 1336−1340.
(28) Eisenmann, B.; Hofmann, A. *Z. Kristallogr.* **1991**, *197*, 157−158.
(29) Eisenmann, B.; Hofmann, A. *Z. Kristallogr.* **1991**, *197*, 139−140.

10.1021/ic000210c CCC: $19.00
Published on Web 06/17/2000

formed by sharing two corners of two AlQ_4 tetrahedra are found in the first class of compounds. The second possesses one-dimensional $^1_\infty[AlQ_2^- = AlQ_{4/2}^-]$ chains built up by edge-sharing of AlQ_4 tetrahedra, and alkali metals sit in the square antiprisms between $^1_\infty[AlQ_{4/2}^-]$ chains. The last class of compounds has two-dimensional $^2_\infty[AlQ_6Q_{4/2}^-]$ layers (Q = Se, Te) formed by the fusion of adamantane-like Al_4Q_{10} supertetrahedra.

Our previous systematic investigations in Li−Mn−Q (Q = Se, Te) systems revealed new ternary compounds, $LiMnQ_2$ (Q = Se, Te) with polar layers, $^2_\infty[MnQQ_{3/3}^-]$, though crystallographic data was inadequate to determine the lithium positions in the (likely) presence of lithium disorder.[36−39] Li ions may occupy octahedral sites (as in $NaMnQ_2$; Q = Se, Te) or tetrahedral sites between the $^2_\infty[MnQQ_{3/3}^-]$ layers or in both sites. Since the Al^{III} radius is not much smaller than the effective radius that we observe for Mn^{III}, it is plausible that analogous aluminum compounds could be prepared.[40]

Our investigations in Li−Al−Q (Q = Se, Te) systems yielded new ternary aluminum chalcogenides, $LiAlSe_2$, α-$LiAlTe_2$, and β-$LiAlTe_2$, for which we report the synthesis and characterization.

Experimental Section

Materials and Instrumentation. Because the compounds described herein are sensitive to both moisture and oxygen, experimental operations were carried out under an atmosphere of either nitrogen or argon. Elemental starting materials Al (99.95%, Aldrich), Te (99.997% Aldrich), Se (99.999%, Aldrich), and Li (99.9%, Aldrich) were used as received. Li_2S, Li_2Se, and Li_2Te were synthesized in liquid NH_3 as described in the literature.[41,42] Binary starting materials Al_2Te_3, Al_7Te_{10}, and Al_2Se_3 were prepared in silica tubes as described in the literature.[43−45] After syntheses, the purity of these starting binary chalcogenides was monitored by examination of Guinier X-ray powder patterns. Atomic absorption (AA) measurements were performed on a Varian SpectrAA 250 Plus instrument after dissolution of products in 20% (w/w) nitric acid. Samples for AA measurements were gathered by selecting crystals from the reaction products. Standard solutions for AA measurements were purchased from Aldrich. For each element, measurements on at least three standard solutions were taken with different concentrations to obtain a linear calibration plot. Wavelength-dispersive X-ray spectrometry (WDS) analyses were performed using a Cameca SX 50 electron microprobe equipped with four WDS spectrometers. Each spectrometer contains an X-ray diffraction crystal as a monochromator and a gas-flow proportional ionization detector. For each element analyzed, a well-characterized compound or pure element is used as a standard. Crystals of ternary compounds were mounted on the top of sample holders with double-sided carbon tape. For each compound, measurements were performed at least three times for independent crystals, and analyses were processed through the Cameca PAP full-quantitative matrix correction program.[46]

Room temperature ^7Li MAS NMR spectra were recorded on a Bruker ACP-300 spectrometer at 116.59 MHz and 4.3 kHz spinning rate. Samples were placed into Zirconia (o.d. 7 mm) rotors and spun using a Bruker supplied solid-state accessory. The lithium spectra were referenced to a 1 M LiCl aqueous solution.

Synthesis. Unless otherwise indicated, all ternary aluminum chalcogenides were synthesized by the use of Nb tubes that were in turn sealed in evacuated (~10^{-4} Torr) silica tubes. $LiAlSe_2$ was synthesized by mixing Li, Al_2Se_3, and Se in a stoichiometric ratio. The temperature was uniformly raised from room temperature to 250 °C over 12 h, held at that temperature for 2 days, raised to 800 °C over 48 h, held at that temperature for 10 days, then cooled to 350 °C at a rate of 2 °C/h, and finally quenched to room temperature. Products contained colorless transparent single crystals suitable for X-ray crystallography.

Pale-gray transparent α-$LiAlTe_2$ was synthesized directly using Li, Al, and Te combined in a 1:1:2 ratio. The temperature of the reaction vessel was uniformly raised to 500 °C over 2 days, maintained at 500 °C for 2 days, uniformly increased to 800 °C over 2 days, maintained at that temperature for 10 days, then cooled to room temperature.

β-$LiAlTe_2$ was synthesized by mixing Li, Al_2Te_3, and Te in a 2.4:1:1.2 molar ratio. The temperature was uniformly raised to 500 °C over 2 days, maintained at 500 °C for 2 days, uniformly increased to 800 °C for 2 days, maintained at that temperature for 10 days, cooled to 350 °C at a rate of 2 °C/h, and then quenched. The X-ray powder pattern of the final product showed the existence of β-$LiAlTe_2$ (ca. 60%) with Li_2Te and unknown phases. Pale-brown transparent crystals suitable for X-ray studies could be physically separated.

Microprobe analyses on selected crystals from each compound showed approximate compositions $Li_xAl_{1.06(8)}Se_2$, $Li_xAl_{0.97(1)}Te_2$, and $Li_xAl_{1.06(9)}Te_2$ for $LiAlSe_2$, α-$LiAlTe_2$, and β-$LiAlTe_2$, respectively. No other elements heavier than Na, including Nb, were found. AA measurements gave the compositions $Li_{1.07(2)}Al_{0.96(5)}Se_2$, $Li_{0.95(3)}Al_{0.98(4)}Te_2$, and $Li_{1.11(5)}Al_{1.05(3)}Te_2$ for $LiAlSe_2$, α-$LiAlTe_2$, and β-$LiAlTe_2$, respectively.

X-ray Crystallography. X-ray diffraction data for $LiAlSe_2$, α-$LiAlTe_2$, and β-$LiAlTe_2$ were collected on a Siemens R3m/V diffractometer with graphite monochromated Mo Kα radiation (λ = 0.710 73 Å) at 20 °C. Cell constants and an orientation matrix for each compound were obtained from a least-squares refinement using the setting angles from at least 15 centered reflections from the rotational photograph. Cell parameters were refined by centering on at least 24 reflections in the range $15 \le 2\theta \le 45°$. Three check reflections were monitored every 97 reflections throughout the data collection process in each compound. The data were corrected for absorption using the ψ-scan technique based on at least five reflections. Structure refinements were based on F^2 with the use of the SHELX-93 package of programs.[47] Reported cell parameters were refined from Guinier powder diffraction patterns using Si as an internal standard.

A colorless transparent crystal of $LiAlSe_2$ having approximate dimensions 0.08 mm × 0.06 mm × 0.06 mm was mounted in a glass capillary. A hemisphere of data ($\pm h, +k, \pm l$) was collected by use of $\theta-2\theta$ scans with $2\theta < 51°$. A total of 374 reflections are unique, and 295 reflections with $I > 2\sigma(I)$ were used in the refinements. Systematic absences, Guinier X-ray diffraction data, and elemental analysis suggested that $LiAlSe_2$ is isostructural with the known compound $LiInSe_2$ (orthorhombic space group $Pna2_1$), so the atomic positions of $LiInSe_2$ were used to begin refinement of the $LiAlSe_2$ structure.[22] Final anisotropic refinement of $LiAlSe_2$ gave 3.07 and 6.42% for final $R(F)$ and $wR2(F^2)$ with $I > 2\sigma(I)$. The largest remaining peaks in the final

(30) Eisenmann, B.; Hofmann, A. *Z. Kristallogr.* **1991**, *197*, 173−174.
(31) Eisenmann, B.; Hofmann, A. *Z. Kristallogr.* **1991**, *197*, 151−152.
(32) Eisenmann, B.; Hofmann, A. *Z. Kristallogr.* **1991**, *197*, 161−162.
(33) Eisenmann, B.; Hofmann, A. *Z. Kristallogr.* **1991**, *197*, 171−172.
(34) Eisenmann, B.; Hofmann, A. *Z. Kristallogr.* **1991**, *197*, 141−142.
(35) Kim, J.; Hughbanks, T. *J. Solid State Chem.* **2000**, *149*, 242−251.
(36) Wang, C.; Kim, J.; Hughbanks, T. In *Materials Research Society Symposium Proceedings*; Jacobson, A., Davies, P., Vanderah, T., Torardi, C., Eds.; Materials Research Society: Boston, MA, 1997; Vol. 453, pp 23−28.
(37) Kim, J.; Wang, C.; Hughbanks, T. *Inorg. Chem.* **1998**, *37*, 1428−1429.
(38) Kim, J.; Wang, C.; Hughbanks, T. *Inorg. Chem.* **1999**, *38*, 235−242.
(39) Kim, J.; Hughbanks, T. *J. Solid State Chem.* **1999**, *145*, 217−225.
(40) Pauling, L. *The Nature of the Chemical Bond*, 3rd ed.; Cornell University Press: Ithaca, New York, 1960.
(41) Feher, F. In *Handbuch der Präparativen Anorganischen Chemie*; Brauer, G., Ed.; Ferdinand Enke Verlag: Stuttgart, Germany, 1954.
(42) Klemm, W.; Sodomann, H.; Langmesser, P. *Z. Anorg. Allg. Chem.* **1939**, *241*, 281−304.
(43) Nesper, R.; Curda, J. *Z. Naturforsch* **1987**, *42b*, 557−564.
(44) Conrad, O.; Schiemann, A.; Krebs, B. *Z. Anorg. Allg. Chem.* **1997**, *623*, 1006−1010.
(45) Schneider, V. A.; Gattow, G. *Z. Anorg. Allg. Chem.* **1954**, *277*, 49−59.
(46) Pouchou, J. L.; Pichoir, F. *Rech. Aerosp.* **1984**, *3*, 13−38.
(47) (a) Sheldrick, G. M. *SHELXTL-93 User Guide*; Crystallography Department, University of Göttingen: Göttingen, Germany, 1993. (b) *SHELXTL-93 User Guide*, version 3.4; Nicolet Analytical X-ray Instruments: Göttingen, Germany, 1993.

Table 1. Crystallographic Data for $LiAlSe_2$, α-$LiAlTe_2$, and β-$LiAlTe_2$

chemical formula	$LiAlSe_2$	α-$LiAlTe_2$	β-$LiAlTe_2$
a, Å	6.8228(9)	6.3517(4)	4.4810(6)
b, Å	8.266(1)		
c, Å	6.5236(7)	11.6904(9)	7.096(1)
V, Å^3	367.90(8)	471.64(6)	123.39(3)
Z	4	4	1
fw	191.84	289.12	289.12
space group	$Pna2_1$ (No. 33)	$I\bar{4}2d$ (No. 122)	$P3m1$ (No. 156)
temp, °C	20	20	20
λ, Å	0.710 73	0.710 73	0.710 73
ρ_{calcd}, g/cm^3	3.463	4.072	3.891
μ, mm^{-1}	20.061	12.340	11.793
R_1[a], wR2[b] [$I \geq 2\sigma(I)$]	0.0307, 0.0642	0.0193, 0.0424	0.0199, 0.0378
R_1[a], wR2[b] (all data)	0.0477, 0.0690	0.0210, 0.0433	0.0262, 0.0433

[a] $R_1(F) = \sum(||F_o| - |F_c||)/\sum(|F_o|)$. [b] $wR2(F^2) = [\sum|w(F_o^2 - F_c^2)^2|/\sum|w(F_o^2)^2|]^{1/2}$, $w = 1/[\sigma^2(F_o^2) + (xP)^2 + yP]$ where $P = (\max(F_o^2,0) + 2F_c^2)/3$. $x = 0.024$ and $y = 0.0$ for $LiAlSe_2$, $x = 0.028$ and $y = 0.0$ for α-$LiAlTe_2$, and $x = 0.0$ and $y = 0.5387$ for β-$LiAlTe_2$.

Fourier difference map were 1.122 e/Å^3 located close to Se1 (0.99 Å) in the framework of the structure.

A pale-gray transparent crystal of α-$LiAlTe_2$ with approximate dimensions 0.10 mm × 0.10 mm × 0.30 mm was selected and mounted in a glass capillary. Data were collected in one quadrant ($+h$, $+k$, $\pm l$) in the $\theta-2\theta$ scanning mode for reflections with $7 \leq 2\theta \leq 51°$. Data for which $h + k + l = 2n + 1$ were systematically absent, consistent with a body-centered tetragonal space group. A total of 138 reflections were unique, and 126 reflections with $I > 2\sigma(I)$ were used in the refinements. α-$LiAlTe_2$ is isostructural with $LiInTe_2$, so the atomic positions of $LiInTe_2$ were used to begin refinement.[21] Final anisotropic refinement gave 1.93 and 4.24% for final $R(F)$ and $wR2(F^2)$ with $I > 2\sigma(I)$. The largest residual peak in the final Fourier difference map was 0.885 e/Å^3, located close to Te in the framework of the structure.

A pale-brown transparent crystal of β-$LiAlTe_2$ with approximate dimensions 0.10 mm × 0.10 mm × 0.10 mm was selected and mounted in a glass capillary. Intensity data were collected in the $\theta-2\theta$ scanning mode for reflections with $5 \leq 2\theta \leq 60°$. One hemisphere of data ($+h$, $\pm k$, $\pm l$) was collected. A total of 170 reflections were unique and used in the refinements. An initial structural model for refinement was found by direct methods. Isotropic refinement of the structure with all Li, Al, and Te positions fully occupied resulted in a residual (R) of 5.13%. In the last cycle, the structure was refined anisotropically to yield respective residuals of 1.99 and 3.78% for $R(F)$ and $wR2(F^2)$ for data with $I > 2\sigma(I)$. The largest remaining peak in the final Fourier difference map was 1.384 e/Å^3 located near Te1 (0.65 Å) in the framework of the structure. A summary of crystal and data collection parameters of $LiAlSe_2$, α-$LiAlTe_2$, and β-$LiAlTe_2$ is listed in Table 1 and final atomic coordinates are shown in Table 2.

Results and Discussion

Syntheses. $LiAlSe_2$ was first obtained from reactions intended to produce a compound isostructural with $LiMnSe_2$.[39] A 2:1:1 mixture of Li, Al_2Se_3, and Se was reacted in a Nb container at 700 °C for 4 days. Guinier X-ray powder patterns showed that the products were mixtures of the major product $LiAlSe_2$ and minor unknown phases. To optimize conditions for $LiAlSe_2$ synthesis, starting materials (several combinations of elements Li, Al, Se and binaries Li_2Se, Al_2Se_3), reaction temperatures (700, 800, and 900 °C), cooling speed (from quenching at reaction temperature to slow cooling (2 °C/h)), and reaction containers (Nb and silica) were varied. Several experiments revealed that the most important factors for the successful synthesis of $LiAlSe_2$ are reaction time and temperature. Longer reaction times (>10 days) and appropriate reaction temperatures (800 °C) are required to yield pure white $LiAlSe_2$. Lower reaction temperature (700 °C) and short reaction time (<5 days) gave significant amounts of unknown phases. Undesirable reaction between the Nb container and Se occurs at 900 °C, as was discussed in a previous paper.[39] Nb containers are otherwise preferred for easy recovery and higher purity of products, as indicated in powder patterns of the products. Attempts to find other phases in the Li−Al−Se system by changing loading stoichiometry nevertheless yielded $LiAlSe_2$ as the major ternary phase.

Table 2. Atomic Coordinates and Equivalent Isotropic Displacement Parameters

atom	position	*x*	*y*	*z*	U_{eq}[a] (Å^2 × 10^3)
			$LiAlSe_2$		
Se1	4*a*	0.0637(2)	0.1152(2)	0.6337(7)	10(1)
Se2	4*a*	0.4067(2)	0.1371(2)	0.1131(7)	10(1)
Al	4*a*	0.0735(5)	0.1256(7)	0.0	9(1)
Li	4*a*	0.085(4)	0.619(5)	0.003(5)	26(6)
			α-$LiAlTe_2$		
Li	4*b*	0.0	0.0	0.5	29(7)
Al	4*a*	0.0	0.0	0.0	15(1)
Te	8*d*	0.2308(1)	1/4	1/8	17(1)
			β-$LiAlTe_2$		
Te1	1*c*	2/3	1/3	0.1257(9)	27(1)
Te2	1*b*	1/3	2/3	0.6173(9)	27(1)
Al	1*b*	1/3	2/3	0.0	28(1)
Li	1*a*	0.0	0.0	0.400(6)	42(1)

[a] Equivalent isotropic U defined as one-third of the trace of the orthogonalized U_{ij} tensor.

Our investigations have uncovered two polymorphs of $LiAlTe_2$ (α and β). α-$LiAlTe_2$ was first synthesized directly from elemental starting materials Li, Al, and Te in sealed Nb tubes at 800 °C. Careful investigations of X-ray patterns revealed that the reaction products contain α-$LiAlTe_2$ as a major compound and a small amount (ca. 5−10%) of unknown phase that was later identified as β-$LiAlTe_2$. After structural characterization of α-$LiAlTe_2$, further reactions were conducted to optimize the yield of β-$LiAlTe_2$ in which several parameters were varied (starting materials, reaction temperatures, cooling speed, reaction containers). Silica tubes were reactive toward starting materials (Li_2Te and Li) and sometimes did not survive the reactions. Therefore, the syntheses of ternary lithium aluminum tellurides were conducted in Nb containers. Surprisingly, we observed that the use of Li, Al_2Te_3, and Te as starting materials produced β-$LiAlTe_2$ as a major product (60%) with Li_2Te and some unknown phases. However, several subsequent attempts to produce pure β-$LiAlTe_2$ were unsuccessful. To understand this polymorphism (α- and β-$LiAlTe_2$), we investigated the factors controlling the formation of the two different compounds. The results are summarized in Scheme 1.

When elemental starting materials were used, Al_7Te_{10} (a compound in which an $Al^{II}-Al^{II}$ bond is present)[43] was identified as a major intermediate phase in the synthesis of pure α-$LiAlTe_2$. Al_7Te_{10} was observed by quenching the reaction after 100 h at 800 °C (Scheme 1a). When Al_2Te_3, Li, and Te were used as starting materials, Al_2Te_3 and Li_2Te were found as the intermediate phases in the synthesis of β-$LiAlTe_2$ (Scheme 1b), as determined by quenching the reaction after 100 h at 800 °C. Thus, different products are formed via different intermediates when the starting materials are different. Syntheses of α-$LiAlTe_2$ and β-$LiAlTe_2$ were reproduced by use of intermediate phases as the starting materials: Li_2Te, Al_7Te_{10}, and Te for α-$LiAlTe_2$ and Li_2Te and Al_2Te_3 for β-$LiAlTe_2$ (see Scheme 1). As was shown for ternary manganese tellurides,[38] elemental Te can react with Nb containers to form binary phases (NbTe and Nb_5Te_4), which favors the formation of a Te-deficient binary intermediate such as Al_7Te_{10} rather than Al_2Te_3 for the synthesis of α-$LiAlTe_2$. We therefore suspect that α-$LiAlTe_2$ is Te-

Scheme 1

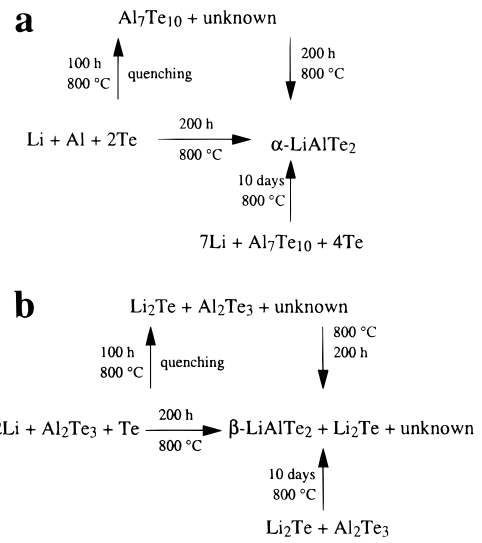

deficient (α-$LiAlTe_{2-\delta}$), although such a deficiency must be too small to be detected in elemental analyses (WDS and AA) or by X-ray crystallography. However, the conversion of α-$LiAlTe_2$ to β-$LiAlTe_2$ by adding excess Te in either silica tubes or Nb containers at 800 °C was not achieved. β-$LiAlTe_2$, along with Li_2Te and unknown phases, is preferably formed from binary tellurides (Li_2Te and Al_2Te_3), which are less reactive toward Nb containers. Despite several thermal treatments at 800 °C over several days in either silica or Nb containers, interconversion of α-$LiAlTe_2$ and β-$LiAlTe_2$ was not observed.

Interestingly, $AgAlS_2$-I and $AgAlS_2$−II (high-pressure phase) are isostructural with α-$LiAlTe_2$ and β-$LiAlTe_2$, respectively.[10,12,13,48] Tetragonal $AgAlS_2$-I is converted to hexagonal $AgAlS_2$-II at 350 °C and 25 kbar.

These ternary aluminum chalcogenides are quite air- and moisture-sensitive. $LiAlSe_2$ decomposes to form malodorous H_2Se and red elemental Se on contact with air. H_2Te and black elemental Te are formed on the decomposition of both α- and β-$LiAlTe_2$.

Structure. Thermal ellipsoid and polyhedral representations of $LiAlSe_2$ (β-$NaFeO_2$-type structure) are projected down the *a* axis in Figure 1. Selected interatomic distances and angles are listed in Table 3. This structure is a superstructure of wurtzite with quadrupled cell volume. The metrical relationships between the hexagonal structure of wurtzite and the ideal orthorhombic superstructure of $LiAlSe_2$ are

$$a_w = c_o/\sqrt{8/3} = a_o/\sqrt{3} = b_o/2$$

where a_w is the *a* axis of wurtzite and c_o, a_o, and b_o are cell parameters of the orthorhombic lattice of the $LiAlSe_2$ structure. In the true $LiAlSe_2$ structure, the *b* axis is somewhat elongated (3.5%) in comparison with the ideal wurtzite structure. In $LiAlSe_2$, $AlSe_4$ tetrahedra are slightly distorted and each tetrahedron shares four corners with four adjacent tetrahedra in forming the three-dimensional structure (Figure 1). Al−Se distances range from 2.366(5) to 2.392(5) Å, and angles are between 107.2(2) and 112.8(2)°. Li cations sit in the tetrahedral holes in the same layers of aluminum with Li−Se distances ranging between 2.55(2) and 2.57(3) Å. Attempts to locate Li in the other possible tetrahedral or octahedral holes were unsuccessful.

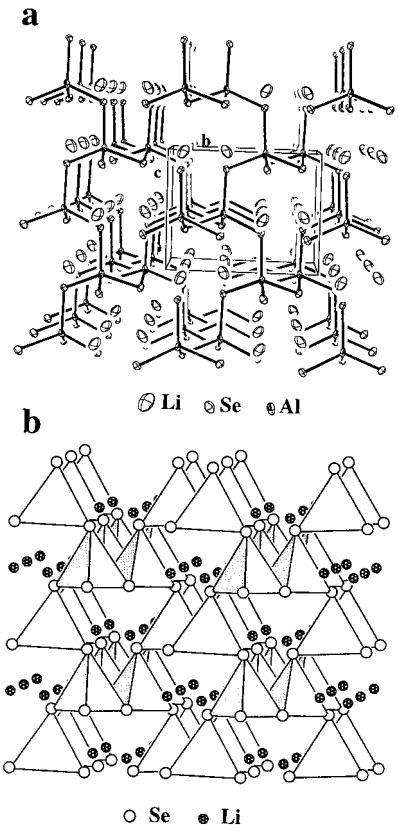

Figure 1. (a) [100] projection of thermal ellipsoid plot of $LiAlSe_2$. 70% probability ellipsoids are shown. (b) Polyhedral representation of $LiAlSe_2$ viewed down the *a* axis, where bonds between Li and Se were removed for clarity, white open circles are Se atoms, and shaded circles are Li atoms.

Table 3. Important Interatomic Distances (Å) and Bond Angles (deg) for $LiAlSe_2$, α-$LiAlTe_2$, and β-$LiAlTe_2$

	$LiAlSe_2$		
Al−Se1	2.392(5)	Se2−Al−Se1	109.0(2)
Al−Se1	2.366(5)	Se1−Al−Se1	109.1(2)
Li−Se1	2.55(2)	Se2−Al−Se1	109.7(2)
Al−Se2 (×2)	2.387(4)	Se2−Al−Se1	112.8(2)
Li−Se2 (×2)	2.55(4)	Se2−Al−Se2	109.1(2)
Li−Se1	2.57(3)	Se1−Al−Se2	107.2(2)
	α-$LiAlTe_2$		
Al−Te (×4)	2.6087(4)	Te−Al−Te (×4)	108.29(1)
Li−Te (×4)	2.7534(4)	Te−Al−Te (×2)	111.87(1)
	β-$LiAlTe_2$		
Al−Te1 (×3)	2.741(2)	Te1−Al−Te1 (×3)	109.7(1)
Al−Te2	2.716(6)	Te1−Al−Te2 (×3)	109.3(1)
Li−Te1 (×3)	3.23(3)		
Li−Te2 (×3)	3.01(2)		

Thermal ellipsoid and polyhedral depictions of α-$LiAlTe_2$ viewed down the *b* axis are shown in Figure 2, and selected interatomic distances and angles are listed in Table 3. α-$LiAlTe_2$ adopts the chalcopyrite ($CuFeS_2$) structure type, consisting of fairly regular $AlTe_4$ tetrahedral building blocks (d(Al−Te) = 2.6087(4) Å (×4) and ∠(Te−Al−Te) = 108.29(1)° (×4), 111.87(1)° (×2)). Each Te atom is two-coordinate with respect to Al, and the [$AlTe_2$] network is, once again, three-dimensional. Li cations occupy tetrahedral holes (d(Li−Te) = 2.7534(4) Å (×4)) within this network. While selenium atoms are hexagonally close packed in $LiAlSe_2$, tellurium atoms form a cubic closed packing in α-$LiAlTe_2$. Factors determining structural choice between β-$NaFeO_2$ ($LiAlSe_2$) type and chalcopyrite (α-

(48) Range, K.; Engert, G.; Weiss, A. *Z. Naturforsch.* **1974**, *29b*, 186−189.

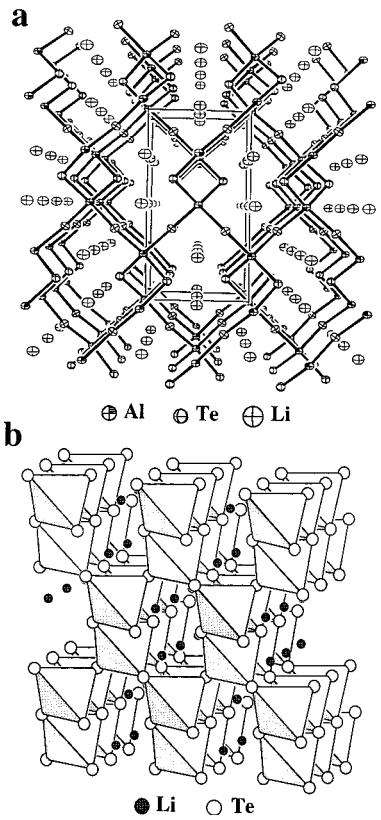

Figure 2. [100] projection of thermal ellipsoid plot (a) and polyhedral representation (b) of α-$LiAlTe_2$. 70% probability ellipsoids are shown. Bonds between Li and Te were removed for clarity. White open circles are Se atoms, and shaded circles are Li atoms in part b.

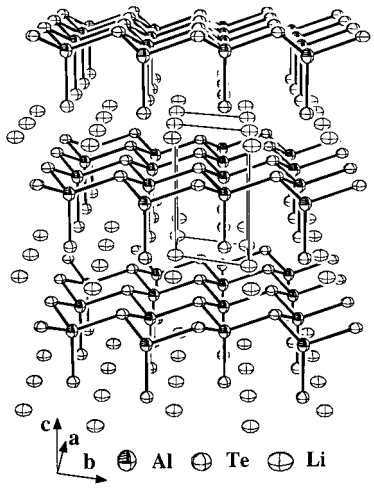

Figure 3. Thermal ellipsoid plot of β-$LiAlTe_2$ along the *c* axis. 70% probability thermal ellipsoids are shown.

$LiAlTe_2$) are not clear, but apparently the size of chalcogenides is important. The same trends are seen in ternary indium chalcogenides $LiInQ_2$ (Q = S, Se, Te) in which sulfide and selenide adopt the β-$NaFeO_2$ structure type, but the telluride shows a chalcopyrite structure.[14,21−23,25] This trend is also evident in the ternary pnictide family $A^{II}B^{IV}C^{V}_2$ (A = Be, Mg, Mn, Cd, Zn; B = Si, Ge, Sn; C = N, P, As) in which ternary nitrides adopt β-$NaFeO_2$ ($LiAlSe_2$) type while phosphides and arsenides adopt the chalcopyrite (α-$LiAlTe_2$) structure type.[16,19,20,49−62]

The crystal structure of β-$LiAlTe_2$ is shown in Figure 3, and selected interatomic distances and angles are listed in Table 3. Like the isostructural $LiMnTe_2$, β-$LiAlTe_2$ has polar layers, $^2_\infty[AlTeTe_{3/3}^-]$ with *d*(Al−Te1) = 2.741(2) Å (×3) and *d*(Al−Te2) = 2.716(6) Å. Li atoms are located in the distorted trigonal antiprisms between layers, having Li−Te distances 3 × 3.23(2) Å (Te1) and 3 × 3.01(3) Å (Te2). The structure of β-$LiAlTe_2$ may also be viewed as inverse $ScCuS_2$ and $AgAlS_2$-II (high-pressure phase) where Cu^I and Ag^I are in the tetrahedral sites and Sc^{III} and Al^{III} occupy the octahedral sites.[48,63] The shortest Te−Te contact in β-$LiAlTe_2$ is 4.4810(6) Å.

Li positions in β-$LiAlTe_2$ are unambiguously determined, which contrasts with the situation for $LiMnTe_2$ (where it was not possible to determine Li positions). A possible explanation for the difference may be that the bigger manganese atoms produce larger tetrahedral and octahedral holes between the layers. This enlarged volume may enable mobility of Li cations or engender static disorder over both octahedral and tetrahedral sites.

Room temperature ^{7}Li MAS NMR measurements were performed for ternary lithium aluminum chalcogenides. Chemical shifts in the spectra have often proved to provide characteristic information regarding local environments of lithium atoms.[64−67] Unfortunately, chemical shifts of lithium atoms in ternary and binary chalcogenides are relatively insensitive to both the coordination number and chalcogen atoms coordinated. The ^{7}Li spectra for $LiAlSe_2$, α-$LiAlTe_2$, and β-$LiAlTe_2$ show a single resonance at 1.26, 2.23, and 0.50 ppm, respectively. These chemical shifts are comparable to 2.06 (Li_2S), 1.69 (Li_2Se), and 0.95 ppm (Li_2Te) for lithium chalcogenides.

Concluding Remarks

The ternary aluminum chalcogenides $LiAlSe_2$, α-$LiAlTe_2$, and β-$LiAlTe_2$ have been synthesized and characterized by the use of single-crystal and powder X-ray diffraction, microprobe analyses, atomic absorption measurements, and ^{7}Li MAS NMR spectroscopy. All these ternary compounds possess different structures despite being built with the same AlQ_4 (Q = Se, Te) tetrahedra. Structural investigations on ternary lithium chalcogenides of aluminum and manganese show that chalcogen atoms are stacked with either ccp (α-$LiAlTe_2$) or hcp ($LiMnQ_2$ (Q = Se, Te), $LiAlSe_2$, and β-$LiAlTe_2$) eutaxies. Al^{III} and Mn^{III} are located in the tetrahedral holes between the chalcogen layers,

(49) Eckerlin, V. P.; Rabenau, A.; Nortmann, H. *Z. Anorg. Allg. Chem.* **1967**, *353*, 114−121.
(50) Wintenberger, M.; Marchand, R.; Maunaye, M. *Solid State Commun.* **1977**, *21*, 733−735.
(51) Pfister, V. H. *Acta Crystallogr.* **1958**, *11*, 221−224.
(52) Folberth, V. O. G.; Pfister, H. *Acta Crystallogr.* **1961**, *14*, 325−326.
(53) Abrahams, S. C.; Berstein, J. L. *J. Chem. Phys.* **1971**, *55*, 796−803.
(54) Honle, W.; von Schnering, H. G. *Z. Kristallogr.* **1981**, *155*, 319−320.
(55) Grigorovici, R.; Mănăilă, R. *Acta Crystallogr.* **1968**, *B24*, 535−541.
(56) Levalois, M.; Allais, G. *Phys. Status Solidi.* **1988**, *109a*, 111−119.
(57) Abrahams, S. C.; Berstein, J. L. *J. Chem. Phys.* **1970**, *52*, 5607−5613.
(58) Wintenberger, M.; Guyader, J.; Maunaye, M. *Solid State Commun.* **1972**, *11*, 1485−1488.
(59) Wintenberger, M.; Tcheou, F. *Z. Naturforsch.* **1980**, *35b*, 604−608.
(60) Vaipolin, A. A.; Grryunnova, N. A.; Kleshchinskii, L. I.; Loshakova, G. V.; Osmanov, E. O. *Phys. Status Solidi.* **1968**, *29*, 435−443.
(61) Wintenberger, M. *Mater. Res. Bull.* **1973**, *8*, 1049−1054.
(62) Lind, M. D.; Grant, R. w. *J. Chem. Phys.* **1973**, *58*, 357−362.
(63) Dismukes, J. P.; Smith, R. T. *J. Phys. Chem. Solids* **1971**, *32*, 913−922.
(64) Menetrier, M.; Rougier, A.; Delmas, C. *Solid State Commun.* **1994**, *90*, 439−442.
(65) Eckert, H.; Zhang, Z.; Kennedy, J. H. *Chem. Mater.* **1990**, *2*, 273−279.
(66) Lee, J. Y.; Wang, F.; Grey, C. P. *J. Am. Chem. Soc.* **1998**, *120*, 12601−12613.
(67) Stewart, F. F.; Stebbins, J. F.; Peterson, E. S.; Farnan, I.; Dunham, S. O.; Adams, E.; Jennings, P. W. *Chem. Mater.* **1995**, *7*, 363−367.

and Li^+ is in either tetrahedral holes ($LiAlSe_2$ and α-$LiAlTe_2$) or octahedral holes (β-$LiAlTe_2$).

Acknowledgment. This research was generously supported by the Texas Advanced Research Program through Grant 010366-097. The R3m/V single-crystal X-ray diffractometer and crystallographic computing system were purchased from funds provided by the National Science Foundation (Grant CHE-8513273). We thank Dr. Renald Guillemette, Dr. Anatoly Bortun, and Dr. Robert Taylor for their assistance with the microprobe analyses, atomic absorption measurements, and ^7Li MAS NMR studies.

Supporting Information Available: Figures S1 and S2 showing ^7Li MAS NMR spectra for ternary and binary lithium chalcogenides, and CIF files containing data for the structures of $LiMnSe_2$, α-$LiAlTe_2$, and β-$LiAlTe_2$. This material is available free of charge via the Internet at http://pubs.acs.org.

IC000210C